The Inverse Problem for Cardiac Arrhythmias

T. M. Bury,[1,2] K. Diagne,[1,2] D. Olshan,[3] L. Glass,[1] A. Shrier,[1] B. B. Lerman,[3] and G. Bub[1]
[1)]*Department of Physiology, McGill University, Montreal, Quebec, Canada*
[2)]*Joint first authors*
[3)]*Department of Medicine, Division of Cardiology, Weill Cornell Medicine, New York*

(*Electronic mail: thomas.bury@mcgill.ca)

(Dated: 29 October 2023)

A cardiac arrhythmia is an abnormality in the rate or rhythm of the heart beat. We study a type of arrhythmia called a premature ventricular complex (PVC), which is typically benign, but in rare cases can lead to more serious arrhythmias or heart failure. There are three known mechanisms for PVCs: reentry, an ectopic focus, and triggered activity. We develop minimal models for each mechanism and attempt the inverse problem of determining which model (and therefore which mechanism) best describes the beat dynamics observed in an ambulatory electrocardiogram. We demonstrate our approach on a patient who exhibits frequent PVCs and find that their PVC dynamics are best described by a model of triggered activity. Better identification of PVC mechanism from wearable device data could improve risk stratification for the development of more serious arrhythmias.

Despite their remarkable reliability, hearts can develop abnormal rhythms, i.e. cardiac arrhythmias. Some of these are serious and may be life threatening. Others are often benign, and might not even be noticeable until they become evident on an electrocardiogram. Premature ventricular complexes (PVCs) represent one of the most frequent arrhythmias and are found in about half the population when the heartbeat is monitored for 24 hours. Although PVCs are usually benign, in some cases they may impair cardiac function and lead to more serious heart problems. On rare occasions they can even trigger lethal ventricular arrhythmias. From a perspective of nonlinear dynamics, the rhythms observed in patients with frequent PVCs represent a formidable challenge for interpretation and modelling. We describe techniques we are developing to determine mathematical models for PVCs that agree with observed rhythms in individual patients with a long range goal of better identifying patients with frequent PVCs at risk for more serious arrhythmia. This article is in honor of Jürgen Kurths on his 70th birthday and in recognition of his major contributions to nonlinear dynamics and the synchronization of oscillations.

I. INTRODUCTION

Every decade our hearts beat several hundred million times. Although most of these beats originate from the normal sinus pacemaker in the upper chambers (atria) of the heart, in many individuals there are also abnormal beats originating from the lower chambers of the heart (ventricles) interspersed with the normal beats. On an electrocardiogram (ECG), these abnormal beats have a different morphology from the normal beats. They typically occur before an expected normal beat is due to occur, and block the appearance of the next normal beat. We call these beats premature ventricular complexes (PVCs). Other terms used for these beats include ventricular premature beats and premature ventricular contractions.

Although PVCs are usually benign in patients without underlying structural heart disease, they may sometimes precede the onset of more serious arrhythmia or lead to heart failure[1–4]. An early clinical study in patients who had a heart attack and frequent PVCs studied the efficacy of drugs in reducing the incidence of more serious arrhythmia or death. Surprisingly, drugs that reduced the incidence of PVCs increased the risk of serious arrhythmia compared to placebo[5]. In current medical practice, PVC occurrence can be reduced by ablating a region of the heart implicated in PVC generation[6]. The ablation procedure requires a high level of expertise. Further, since PVCs are usually benign in clinical practice it is usual to have minimal treatment or analysis of PVC dynamics.

However, from a basic science perspective, the complexities of PVC dynamics provide a challenge. Early studies identified a large number of different dynamic patterns of PVCs[7–10]. Ideally, we would like to identify the mechanisms of PVC formation in individual patients and use this knowledge to assess the medical significance in each patient. In this article we adopt a strategy of setting parameters in very simple models based on observed dynamics. We then carry out simulation and analysis to compare with observed dynamics. We view this as a step towards developing automatic techniques for the inverse problem – to observe the dynamics in a given patient and to then use the data to set an appropriate model.

Cardiologists identify three main mechanisms for PVC generation[2]. Although a detailed discussion of these mechanisms is necessarily technical, we present the gist of the ideas in an effort to develop minimal mathematical models that can be compared with clinical data. The three mechanisms are:

- **Reentry**. The excitation from the sinus beat travels slowly through abnormal ventricular tissue and then reenters the normal ventricular tissue leading to a PVC[11].

- **Enhanced automaticity (parasystole)**. There is an abnormal pacemaker in the ventricles (a parasystolic focus) that competes with the sinus pacemaker. Although in some individuals the parasystolic focus appears to generate beats at a regular interval independent of the

sinus rhythm (*pure parasystole*), in other cases, there is a hypothetical resetting of the abnormal pacemaker (*modulated parasystole*)[12,13].

- **Triggered activity**. There is a localized abnormal region in the ventricles that will generate a PVC following its excitation. Triggering mechanisms are usually ascribed to physiological mechanisms that lead to reactivation of ionic currents involved with excitation of the heart following their normal inactivation. Technical terms for this reactivation are early afterdepolarization or delayed afterdepolarization[14].

In this article we develop minimal models for these three mechanisms and apply them to the analysis of 20-hour record of a single patient. In this patient, there was a persistent rhythm that occurred over 90% of time in which normal beats and PVCs alternated.

The plan of the paper is as follows. In Section II, we present plots reflecting the observed dynamics in the patient. In Section III, we develop minimal models for each of the proposed three mechanisms. We can use the data to determine parameters in the models. In Section IV we discuss the results. The analysis shows that a single set of parameters cannot be used to model the dynamics over the entire record for any of the models. Fluctuations of parameters in models correspond to physiological changes during the course of the recording. Our analysis provides a strategy for tracking physiological changes over time.

II. CARDIAC RHYTHM DATA

The data is derived from a 56-year-old man with a history of non-obstructive coronary artery disease, hypertension, and frequent and symptomatic PVCs. A 20 hour recording of his cardiac activity was carried out using a Mortara HScribe Holter system with a sampling rate ~~was~~ of 180 Hz. Each beat is ~~automatically identified~~ identified and categorised as either a normal beat (N) or a PVC (V) by a technician in concert with beat recognition software, which is then reviewed by a physician. Figure 1 shows recordings when the patient is in normal sinus rhythm (top trace) and in *bigeminy*, a rhythm with an alternation of N beats and V beats (bottom trace). From the ECG in Fig. 1 we can measure the following intervals. The sinus period t_s is the interval between two consecutive N beats, when there are no intervening V beats. If there is bigeminy, the sinus beat that would be expected after the PVC is blocked in its passage through the heart. Consequently, t_s is estimated from the ECG as one half the VV interval on the ECG or one half the interval between two consecutive N beats that are visible on the ECG. The *coupling interval*, NV is the time from a N beat to a PVC.

Although we often have the impression that our hearts are beating regularly, the sinus rate fluctuates during the course of the day, reflecting the body's response to the environment and the intrinsic feedback control loops controlling the heart[15,16]. Although there is broad interest in the mechanisms of heart rate variability, for the present work, we measure these fluctuations without attempting to analyze their mechanisms.

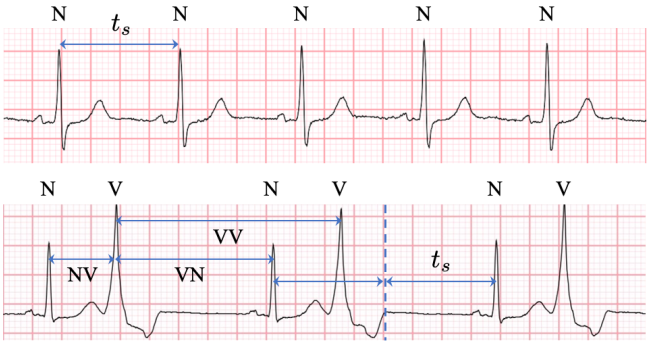

FIG. 1. Electrocardiogram segments from patient of duration 4.4 seconds. Upper panel shows normal sinus rhythm. Lower panel shows a bigeminal rhythm (alternating sinus and ectopic beats). N labels mark sinus beats. V labels mark ectopic beats. t_s is the interval between two sinus beats. During a bigeminal rhythm, the sinus beat following an ectopic beat is blocked (dashed line). The period of the sinus pacemaker (t_s) is approximated has half the time between ectopic beats (VV). The coupling interval (NV) is the time between a sinus beat and the PVC, and the interval (VN) is the subsequent time until the next sinus beat.

The magnitude and variability of the coupling interval from the sinus beat to a PVC, have been reported to have clinical significance[17–19]. In the current case, the coupling interval is $0.467 \pm .028$ s where we give the mean and standard deviation. However, this does not adequately reflect the dynamics observed in this patient. In Fig. 2(a), we give a scatter plot of the coupling interval vs t_s. This data can be fit to a linear regression to obtain

$$NV = 0.21\, t_s + 0.44, \;\; R^2 = 0.23. \tag{1}$$

For any sinus rate, the coupling interval appears to fall in a range of about 100 ms, with an upward trend so that the coupling interval tends to be longer at slower heart rates. A complementary plot, Fig. 2(b), relates VV to VN during bigeminal rhythms. This data can also be fit to a straight line to obtain

$$VV = 1.07\, VN + 0.56, \;\; R^2 = 0.96. \tag{2}$$

Based on the definitions of the intervals in Fig. 1, these expressions are directly related. If $NV = \gamma t_s + \delta$, then

$$VV = \frac{2}{2-\gamma} VN + \frac{2\delta}{2-\gamma}. \tag{3}$$

However, the coefficients in the linear regression do not precisely conform to this relationship, presumably due to the larger affect of noise on the NV interval compared to the VV interval.

In this record, there is structure over short times that is not evident when data for an entire day is aggregated. If we break the record into 5-minute intervals, then the plots of NV vs t_s and VV vs. VN can be fit by a straight line in each segment (Figs. 2(c), 2(d)). In Fig. 3 we give a plot in which we superimpose all the linear regressions of 5-minute intervals. In

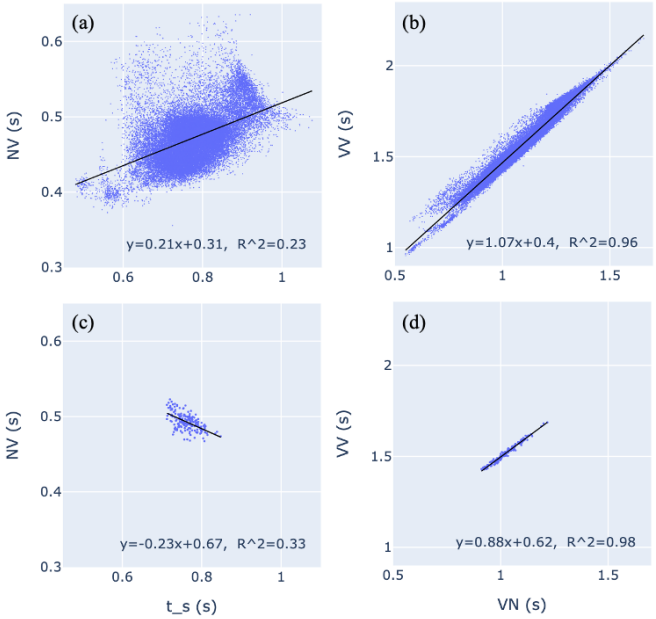

FIG. 2. (a) Coupling interval vs. sinus rate for bigeminal sequence across the entire recording. (b) Phase response plot using the entire recording. (c) Coupling interval vs. sinus rate for bigeminal sequences in a 5-minute segment. (d) Phase response plot of the same 5-minute segment. Black lines and inset text provide linear regressions and R^2 values.

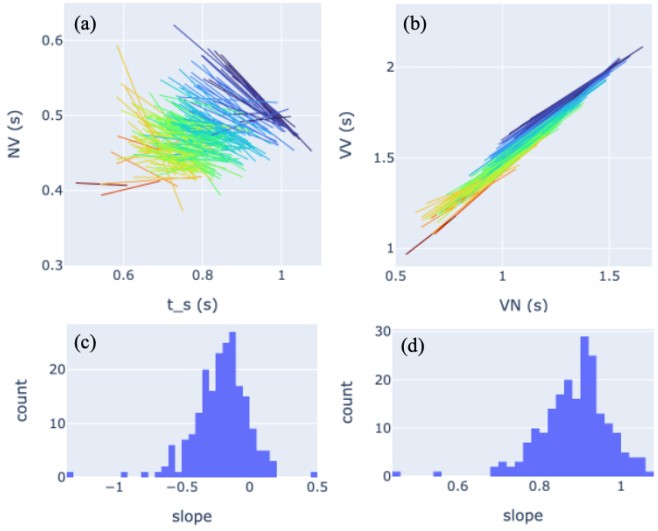

FIG. 3. (a-b) Linear regressions of consecutive, non-overlapping, 5-minute segments of the record. Total of 206 segments that each have ≥ 40 PVCs. Heat of the line corresponds to average t_s which varies from 0.75 s (dark red) to 1.31 s (dark blue). (c-d) Histogram of the slopes from the linear regression.

the NV vs t_s plot, 90% of the time segments have a negative slope, compare with Eq. 1. In the VV vs VN plots, 90% of the time segments have slopes of < 1.0, compare with Eq. 2. The discrepancy between the slopes over short and long intervals is an example of Simpson's paradox[20], in which a trend appears in several groups of data, but is altered, potentially even reversed, when the groups are combined. The bottom panels in Fig. 3 give histograms of the slopes of the linear functions fit to the five minute intervals.

If the correct mechanism for the PVCs was known, then an appropriate theoretical model for the mechanism would necessarily agree with the data in Figs. 2 and 3. In the next section we exploit this notion to set parameters in theoretical models and to eliminate putative theoretical models when the parameters appear to be contrary to physiological expectations.

III. THEORETICAL MODELS FOR PVCS

In this section we pose theoretical models for each of the three mechanisms and carry out simulations with parameters obtained from the clinical data. During the course of the recording, the rhythm was bigeminy with an alternation of PVCs and sinus beats for over 90% of the record. During the record, the sinus rate varied considerably with a period ranging between 0.6–1.2 s.

Changes in the rate of stimulation in cardiac tissue is typically associated with changes in both the velocity of propagation of the cardiac impulse as well as changes in the duration of the excited phase of the cycle (action potential duration). The velocity of propagation depends on the time since the preceding activation. As the time since the preceding activation increases, the velocity increases[21–23]. Similarly, the action potential duration increases as the time since the preceding activation increases. The action potential duration tends to increase as the stimulation frequency decreases[21,24,25]. As a consequence, a slower stimulation frequency leads to a longer action potential duration and a faster velocity of propagation. Although the curves reflecting these dependencies are often represented as exponential functions ,[26], based on the remarkably linear structure observed in Fig. 2 and to facilitate parameter determination based on the data, we will assume linear functions.

A. Reentry

The simplest model for a PVC assumes an anatomical substrate in which the sinus beat encounters a region of unidirectional conduction and a contiguous area of slow conduction that is largely shielded from the bulk of cardiac tissue. Upon exiting the region of slow conduction, the ventricle is reexcited from an abnormal source at the exit point of the slow conduction pathway. We can model this as

$$NV_i = t_{\text{lag}} + \varepsilon_i \tag{4}$$

where NV_i is the time between the ith sinus beat and the subsequent ectopic beat, t_{lag} is the time to travel around the reentrant loop, and ε_i is a noise term which we draw from a normal distribution with mean zero and standard deviation σ. Given that $VV = VN + NV$, we have

$$VV_i = VN_i + t_{\text{lag}} + \varepsilon_i, \tag{5}$$

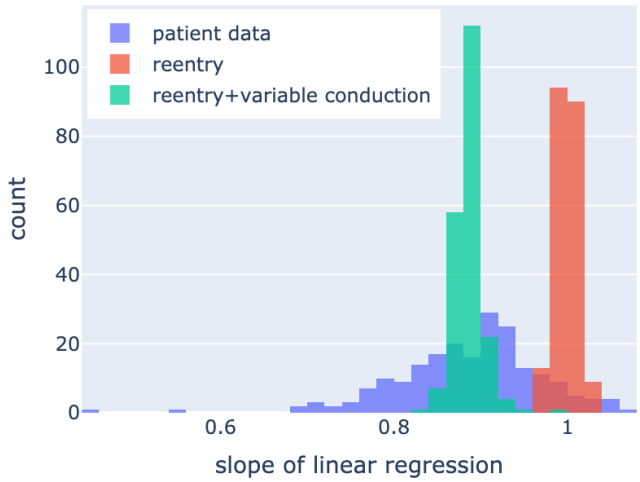

FIG. 4. Histogram ~~showing slope~~ of the slopes of linear ~~regression~~ regressions for each 5-minute ~~segments~~ segment in the patient data (blue), a simulation of the model for reentry with fixed conduction time (red), and a simulation of the model for reentry with variable conduction time (green).

and so the VV-VN plot from this model would have a slope of approximately one. We obtain parameter values from the clinical data as

$$t_{\text{lag}} = \langle VV_i - VN_i \rangle , \tag{6}$$

where $< . >$ takes mean value over all intervals in a bigeminal rhythm. The standard deviation of the noise term σ is set to the mean prediction error of the linear regressions over each 5-minute section, i.e.

$$\sigma^2 = \left\langle \frac{1}{n} \sum_i (\bar{VV}_i - VV_i)^2 \right\rangle , \tag{7}$$

where VV_i is the data, $\bar{VV}_i$ is the prediction from the linear regression, n is the number of data points in the given 5-minute section, and $< . >$ takes the mean over each 5-minute section of the record. We obtain $t_{\text{lag}} = 0.47$ s and $\sigma = 0.012$ s.

We simulate the model based on the VN values that occur during bigeminy in the clinical record. For each VN value, we simulate a VV value using Eq. 5. To compare the output with the clinical data, we compute the linear regression of the VV-VN plot over each 5-minute segment with greater than 40 PVCs, and plot a histogram of the slopes in Fig. 4 (red). Using a t-test (Appendix), we find that 83% of the segments in the clinical data are significantly different from the model simulation ($p < 0.001$).

We now extend this model to allow conduction time across the pathway (t_{lag}) to depend on the time since the pathway was last active (VN). Typically, conduction time is longer when the recovery time is shorter. We model this with the linear ~~relation~~ relationship

$$t_{\text{lag}} = \alpha - \beta\, VN \tag{8}$$

where α and $\beta > 0$ are parameters to be determined. The model becomes

$$VV_i = (1-\beta)\, VN_i + \alpha + \varepsilon_i, \tag{9}$$

which results in a VV-VN plot with slope $1-\beta$. We fit the parameters α and β to the clinical data using the average properties of the linear regressions from each 5-minute interval. The average slope is 0.89, so we set $\beta = 0.11$. We set $\alpha = 0.60$, which is the average intercept. We simulate the model as before, and compute the linear regression over 5-minute segments, plotting the slopes in Fig. 4 (green). This time, we find that 58% of the clinical segments are significantly different from the model simulation ($p < 0.001$). ~~Given this discrepancy, we rule out the model of reentry.~~

B. Pure and modulated parasystole

In pure parasystole, there is an independent pacemaker, also termed an ectopic focus, that competes for control of the heart with the sinus pacemaker and generates PVCs. There are many very specific characteristics of pure parasystole that are not consistent with the current data. For example, for a fixed sinus rate, there tend to be three values for the number of intervening sinus beats between any two PVCs. In contrast, for most of the current record there is only one sinus beat between two PVCs. In addition, the coupling intervals during pure parasystole are quite variable and tend to occur at all coupling intervals between the end of one sinus beat and the start of the next one[9,27,28].

An alternative to pure parasystole is modulated parasystole. In early papers, Moe, Jalife, Antzelevitch and collaborators[11–13] showed that many of the observed patterns of PVCs in patients could be generated if the sinus rhythm reset the PVC. Resetting curves for computations have been based on both experimental and clinical studies. Stimuli early in a cardiac cycle tend to delay the next beat, whereas stimuli later in the cycle tend to advance the next beat[11,13,29–34]. The phase in the PVC cycle at which there is a reversal from lengthening to shortening is called the reversal point, ϕ_c. In the current patient, there is no evidence that the PVC cycle length is increased, and hence we assume that sinus beats that fall before ϕ_c have no effect on the PVC cycle length. Further, following Ikeda[32], we assume that the phase resetting curve, $f(\phi)$ is piecewise linear:

$$f(\phi) = \begin{cases} 1 & 0 \le \phi < \phi_c, \\ 1 + b(\phi - 1) & \phi_c \le \phi < 1, \end{cases} \tag{10}$$

where ϕ is the phase of the sinus beat in the ectopic cycle, and b determines the strength of resetting. A value of $b = 1$ corresponds to immediate resetting of the ectopic cycle. A value of $b = 0$ corresponds to no resetting of the ectopic cycle (pure parasystole). We fix $\phi_c = 0.5$. All phases are taken *modulo* 1.

We use a model for modulated parasystole that incorporates a delay into and out of the ectopic focus (Appendix)[35]. Let ϕ_i

be the phase of the ith sinus beat in the ectopic cycle, then

$$\phi_{i+1} = \begin{cases} \phi_i + \frac{t_s}{t_e} + \frac{\varepsilon_i}{t_e} & 0 \le \phi_i < \frac{t_s-\theta}{t_e} \\ \phi_i + \frac{t_s}{t_e} + 1 - f(\phi_i + \frac{t_{\text{lag}}}{t_e}) + \frac{\varepsilon_i}{t_e} & \frac{t_s-\theta}{t_e} \le \phi_i < 1 \end{cases} \quad (11)$$

where t_s is the sinus cycle length, t_e is the cycle length of the PVC, θ is a refractory period, t_{lag} is the combined time into and out of the site of generation of the PVC, and ε_i is a noise term drawn from a normal distribution.

For values of b close to one and an ectopic cycle length slightly larger than twice the sinus cycle length, the model gives rise to bigeminy, the rhythm observed in the patient. In this case, the model outputs a linear relationship between VV and VN:

$$VV = b\,VN + c \quad (12)$$

where b is as defined earlier and

$$c = b\,t_{\text{lag}} + (1-b)\,t_e. \quad (13)$$

Thus, from a linear regression of the VV-VN plot from the clinical data (Fig. 2(d)), we obtain b directly, and a one-to-one relationship between t_e and t_{lag} (setting one of these parameters determines the other).

Parameters are obtained from the clinical data as follows. The sinus period t_s is computed on a beat by beat basis, and taken as half the local VV interval. The ectopic period $t_e = 2.25$ s is estimated from the longest VV interval over the whole record. The refractory period $\theta = 0.34$ s is estimated from the shortest NV interval over the whole record. The resetting strength $b = 0.89$ and conduction time $t_{\text{lag}} = 0.40$ s are obtained from the average slope and intercept of the linear regressions and using Eq. 13. We simulate the model using Eqs. 10 and 11 for each 5-minute segment of the data. We find that 55% of the clinical segments are significantly different from the model simulation ($p < 0.001$).

C. Triggered activity

Triggered activity is the result of a secondary spike in voltage across the cell membrane known as an afterdepolarization[14]. When an afterdepolarization occurs during the repolarization phase of the action potential, it is referred to as an early afterdepolarization (EAD). If it occurs after repolarization, it is known as a delayed afterdepolarization (DAD). The stimulation frequency can have an effect on the timing and magnitude of afterdepolarizations[36–38], with lower stimulation frequency typically resulting in a longer latency (time between the upstroke of the action potential and the afterdepolarization). This is demonstrated with a simulation of the ToR-ORd[39] model—a detailed ionic model for a human cardiomyocyte. All parameters are as in the original model except for the following which are adjusted by a multiplicative factor to facilitate EADs. The conductance of the rapid delayed rectifier current is decreased to 0.015 times its original value, the conductance of the L-type calcium current is increased to 1.25 times its original value, the recovery time of the L-type calcium current from refractoriness is decreased to 0.4 times its original value, and the conductance of the sodium-calcium exchange current is increased to 1.5 times its original value. These changes are in accordance with understood physiological changes that promote EADs [39,40]. We simulate the model for a range of basic cycle lengths (Fig. 5(a)) and find that the relationship between the latency of the EAD and the basic cycle length is approximately linear (Fig. 5(b)). Therefore, a simple model for triggered activity is

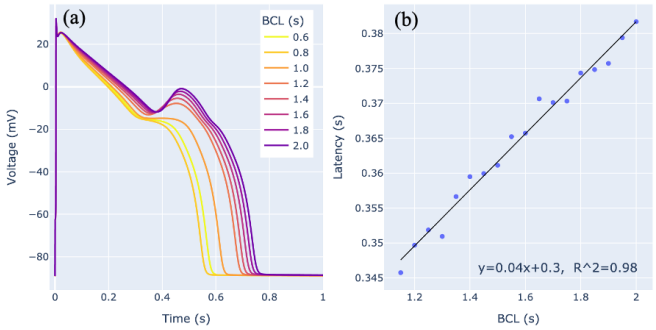

FIG. 5. (a) Simulation of the ToR-ORd[39] computational model for a human cardiac cell at different basic cycle lengths (BCL). To facilitate EADs, the model is set with a reduced rapid late potassium current, an increased L-type calcium current, and an increased sodium-calcium exchange current. (b) Latency (time between upstroke of the action potential and upstroke of the early afterdepolarization) vs. BCL. Inset and line show linear regression.

$$NV_i = \gamma t_s + \delta + \eta_i, \quad (14)$$

where $\gamma > 0$ and δ are the slope and intercept of the linear relationship, respectively, and η_i is a noise term. The model can be rearranged to

$$VV_i = \left(\frac{2}{2-\gamma}\right) VN_i + \frac{2\delta}{2-\gamma} + \varepsilon_i, \quad (15)$$

where $\varepsilon_i = 2\eta_i/(2-\gamma)$. Therefore, this model gives rise to a linear VV-VN relationship with a slope greater than one. While we see a slope of 1.07 across the entire patient record (Fig. 2(b)), the majority of individual 5-minute segments have a slope of less than one. Hence, this model does not give an accurate description of the dynamics.

We now consider a more detailed model that includes a conduction time t_{lag} to and from the site where the afterdepolarization occurs. We use the form as in Eq. 8. We also assume that the latency of the afterdepolarization varies with heart rate, but on a slower timescale. We allow it to vary with t_s averaged over a 5-minute interval, denoted $\langle t_s \rangle$. The model is

$$NV_i = t_{\text{lag}} + g(\langle t_s \rangle) + \varepsilon_i \quad (16)$$

where g is latency of the afterdepolarization, and ε_i is a noise term. As before, we will assume a linear relationship between latency and heart rate:

$$g(\langle t_s \rangle) = \gamma\,\langle t_s \rangle + \delta, \quad (17)$$

where $\gamma > 0$ and δ are the slope and intercept of the linear relationship, respectively. The model may be rearranged to

$$VV_i = bVN_i + c + \gamma\langle t_s\rangle + \varepsilon_i \tag{18}$$

where $b = 1-\beta$ and $c = \alpha + \delta$. On 5-minute time intervals (where $\langle t_s\rangle$ is constant), this model gives a VV vs VN plot with slope less than 1 (since $b < 1$). However, on longer time scales this slope can shift up and down with changes in $\langle t_s\rangle$, similar to what we see in Fig. 3(b).

From the data, we obtain the parameter $b = 0.89$ as before. We obtain $\gamma = 0.42$ as twice the gradient of the global relationship between NV and t_s plotted in Fig. 2(a) (the factor of two arises from the afterdepolarization site being stimulated every other beat). Finally, we obtain $c = 0.37$ by isolating it in Eq. 18 and taking the mean of the resulting expression across the patient data. We simulate the model with these fixed parameters. The linear regressions of the model output are shown in Fig. 6, which appear to be consistent with the data. However, due to the larger variation in the slope of these plots in the clinical data, we find that 53% of the segments in the clinical data are significantly different from the output of the model simulation ($p < 0.001$). ~~This is the best performing model considered.~~

D. Comparing models

For each model, there are are a significant number of segments in the clinical data that are not well described by it. This is likely due to the nonstationarity of the clinical data and our models using fixed parameters to simulate the entire record. Nonetheless, we can compare the relative performance of each model using Akaike's Information Criterion (AIC), which determines the relative goodness of fit of each model and penalises based on the number of parameters that the model uses (Appendix). We compute the AIC score for each model on each 5-minute segment of the clinical data, and find that out of the 206 5-minute segments, the model for triggered activity is best fitting model in 138, the model for modulated parasystole in 48, and the model for reentry in 20.

IV. DISCUSSION

We have studied dynamic properties of an abnormal cardiac rhythm recorded for 20 hours in which there is a persistent rhythm in which normal sinus beats and PVCs alternate. From a cardiology perspective, the main question is whether this rhythm has negative consequences for either the current or future health of the patient and if so, can it be cured. In this instance, the patient was symptomatic, and there was a risk of developing more serious heart problems. The treating physicians undertook an ablation procedure, in which an abnormal region of the heart that appeared to be the source of the rhythm was targeted and destroyed using radiofrequency energy, leading to an elimination of the abnormal rhythm ~~and its resulting symptoms~~(zero PVCs at rest, with isoproterenol, or with up to triple ventricular extra-stimuli in the 45-minute period following the procedure). This success depends on the skill of the physicians in identifying the location of the ablation target (in this case in the "aortic mitral continuity" which is in vicinity of the valve between the left atrium and ventricle), and the ability to maneuver an ablation catheter to this position. A deep understanding of the mechanism of the arrhythmia or a mathematical model of the dynamics was not needed.

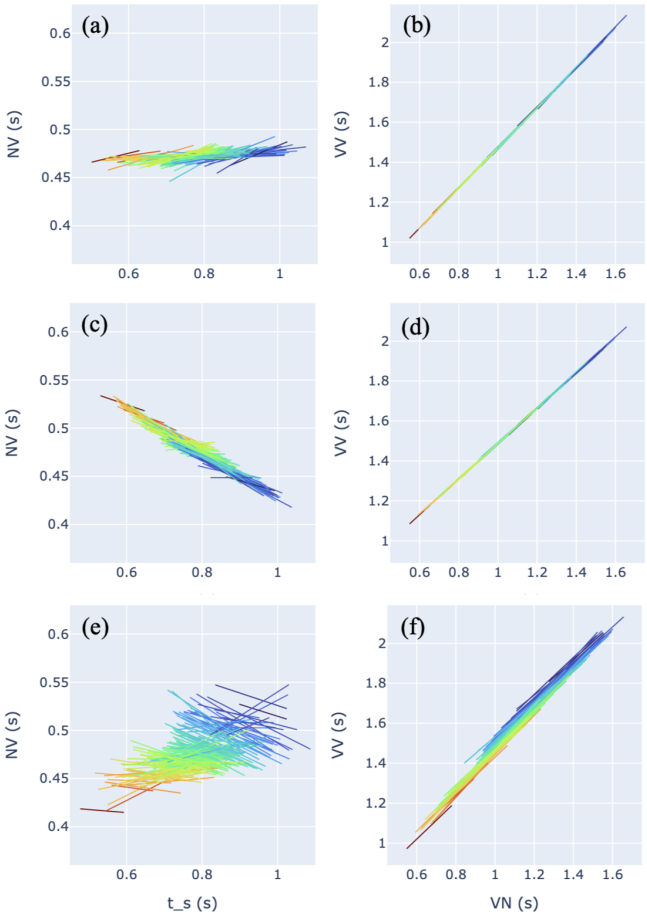

FIG. 6. Linear ~~regressions~~ regression of each 5-minute segment of simulation data from the theoretical model of reentry (a-b), modulated parasystole (c-d) and triggered activity ~~with variable conduction time~~(e-f). ~~Total of~~ Computed on 206 ~~5-min~~ 5-minute segments that each have ≥ 40 PVCs. Heat of the line corresponds to average t_s which varies from 0.75 s (dark red) to 1.31 s (dark blue).

Since there were long periods in which the bigeminy persisted, from a dynamics perspective it appeared to be a very stable rhythm. The simplest way this could happen is if each sinus beat in some fashion had a direct role in the timing of the subsequent PVC. There are several ways in which this could happen. If there was a reentry mechanism then the interval from the sinus beat to the PVC would be equal to the conduction time from point of origin of the sinus beat in the ventricles to site of origin of the PVC. However, since the conduction time in the heart is comparatively fast (the entire ventricle is

activated within 160-200 ms), this is not a plausible mechanism in this patient.

Since experimental and theoretical studies have demonstrated 1:1 phase locking over broad regions of parameter space[13,29,41], before starting the analysis, we thought that a stable 1:1 phase locked rhythm between the sinus rhythm and an autonomous pacemaker was the most likely mechanism for the dynamics in this patient. With this interpretation, the VV vs VN plot, Fig. 2(b), represents the phase resetting curve. Indeed, with the phase resetting curve in Eq. 10, with $b = 0.89$ and the parasystolic period $t_e = 2.13$ s, we would expect to observe bigeminy for the sinus period in the range $0.62\,\text{s} < t_s < 1.065\,\text{s}$. However, the conduction time would be in the range of 250-450 ms, and would increase at the longer sinus cycle times. In view of the rapid conduction time in cardiac tissue and the observation that cardiac conduction velocity tends to increase at lower stimulation frequencies, this mechanism also appears to be incompatible with the observed dynamics.

In contrast, a triggering mechanism due to early or delayed afterdepolarizations has qualitative features that appear consistent with the clinical data. A striking finding is the small but significant increase of the coupling interval at slower heart rates (Fig. 2(a)). Our numerical simulation of the dependence of early afterdepolarizations on the basic cycle length (Fig. 5) showed that coupling interval of afterdepolarizations would be expected to increase as the cycle length increased. Although we do not have a comparable model for delayed afterdepolarizations, the coupling interval of delayed afterdepolarizations is also expected to increase as cycle length increases[38,42].

Over short 5 min intervals, VV vs VN curves usually have a slope less than one, and the NV vs t_s curves tend to have a negative slope. This behavior is consistent with a shortened conduction time from the sinus beat to the ectopic focus at slower cycle lengths provided the timing of the triggered activity is relatively fixed. However, over longer time intervals, we assume that the time of the triggered activity increases as the expected action potential duration increases, for example see[36]. Such a mechanism is also consistent with early clinical observations that relate the occurrence of PVCs to the U-wave a feature on some ECG records that has been ascribed to afterdepolarizations[43]. There is a need for detailed experimental studies that investigate timing and magnitude of afterdepolarizations as a function of stimulation rate.

A triggering mechanism is also consistent with other features of the current record. In this patient there is a strong persistence of the bigeminy. Such persistence was noted at a very early stage, and called the "rule of bigeminy"[10,44]. Since early afterdepolarizations tend to occur at long cycle lengths, the blocked sinus beat after a PVC leads to a mechanism to perpetuate bigeminy once it is started. On the other hand, delayed afterdepolarizations tend to occur at short cycle lengths[14], so it is less clear how they could give persistent bigeminy.

In understanding the origin of PVCs in a patient, an important parameter relates to the conduction time needed for the sinus beat to arrive at the tissue where the PVC originates. In the models for reentry and modulated parasystole, t_{lag} is longer than 0.4 s. This seems quite long, given that the time to activate the entire heart is less than 160 ms in patients with structurally normal hearts. The model for triggered activity yields smaller, more realistic values for t_{lag} since the delay to the PVC consists of the conduction time to the focus and the latency of the afterdepolarization.

In this study, we opted for very simple mathematical models with between only one and three tunable parameters that were fixed during simulations. As such, we do not expect the model simulations to produce similar output to the patient data for every part of the record. Rather, the goal of the models is to capture the qualitative behaviour of the patient, and if not, rule out a particular mechanism. Given the physiological changes that can occur throughout the day, it will be interesting to develop more detailed (nonlinear) models, potentially with time-varying parameters, that better reproduce the clinical record.

Given the evolving technology of wearable devices, data concerning the timing of heartbeats can be measured over long periods of time. In patients who have frequent PVCs, clinicians need to determine if the condition is benign or if it presages progression to a more serious condition. We believe that determination of the mechanism underlying the frequent PVCs will be one important component in assessing appropriate therapy for patients with PVCs. Given the large amount of data concerning the timing of both normal sinus beats and abnormal PVCs in a single patient and the comparative simplicity of the proposed mechanisms for PVC generation, we believe that it should be feasible to determine the values of parameters in an appropriate theoretical model so that the model gives good agreement with observed dynamics, and can then be used to help determine therapy. The realization of this optimistic goal will depend on resolution of the following questions: (i) Are the currently proposed mechanisms for PVC formation adequate, or are there new mechanisms that have not yet been recognized? (ii) Do parameters or perhaps even mechanisms for PVC generation stay constant in time, or change sufficiently slowly for a model to be determined? (iii) Will there be appropriate collaboration between experts in cardiology and nonlinear dynamics in order to determine the mechanisms in individual patients and then use this information to inform medical decision making?

Appendix A: ~~Statistical methods~~Linear regression

To compute the linear regression for a set of data points $\{(x_i, y_i)\}_{i=1}^n$ we use the *linregress* function in the Python package *scipy*, which computes the least-squares regression of the model

$$y_i = \alpha + \beta x_i + \varepsilon_i \tag{A1}$$

to the data, where ε_i is an error term, and α and β are parameters to be fit. We compute the coefficient of determination as the square of the Pearson correlation coefficient r, where

$$r = \frac{\sum_i (x_i - \hat{x})(y_i - \hat{y})}{\sqrt{\sum_i (x_i - \hat{x})^2 \sum_i (y_i - \hat{y})^2}}, \tag{A2}$$

and the circumflex notation is the sample mean. To compare whether the linear regressions of two datasets are significantly different, we use two hypothesis tests. The first, compares the slopes of the linear regression. If the slopes are not found to be significantly different, we then test the intercepts. To test whether the slopes of two datasets, β_1 and β_2, are significantly different we test the following null and alternative hypotheses:

$$\mathrm{H}_0 : \beta_1 = \beta_2, \tag{A3}$$
$$\mathrm{H}_1 : \beta_1 \neq \beta_2. \tag{A4}$$

Under the assumption of the null hypothesis

$$\beta_1 - \beta_2 \sim \mathcal{N}(0, s_{\beta_1}^2 + s_{\beta_2}^2), \tag{A5}$$

where s_{β_1} and s_{β_2} are the standard errors of β_1 and β_2 respectively. To test for a significantly different outcome, we use a two-tailed t-test, with test statistic

$$t = \frac{\beta_1 - \beta_2}{\sqrt{s_{\beta_1}^2 + s_{\beta_2}^2}} \sim T(n_1 + n_2 - 4) \tag{A6}$$

where n_1 and n_2 are the number of data points in each dataset, and T is the Student's t-distribution. If the two slopes are not significantly different i.e. we cannot reject the null hypothesis, then we perform a similar test on the intercepts of the two regressions α_1 and α_2 with the hypotheses

$$\mathrm{H}_0 : \alpha_1 = \alpha_2, \tag{A7}$$
$$\mathrm{H}_1 : \alpha_1 \neq \alpha_2. \tag{A8}$$

If we cannot reject this null hypothesis, then the linear regressions for the two datasets are not significantly different.

Appendix B: Akaike's Information Criterion

To compare relative model performance, we use Akaike's Information Criterion[45], which is given by

$$\mathrm{AIC} = -2\ln(L) + 2k, \tag{B1}$$

where L is the maximum likelihood estimation of the model and k is the number of parameters. In the context of linear regression [46], it can be computed as

$$\mathrm{AIC} = n\ln\left(\frac{\mathrm{SSE}}{n}\right) + 2k, \tag{B2}$$

where SSE is the sum of the squared errors $\sum(\mathrm{VV}_i - \tilde{\mathrm{VV}}_i)^2$ and n is the number of data points. The preferred model is the one with the lowest AIC score.

Appendix C: Model for modulated parasystole with conduction delay

The original model for modulated parasystole with delay[35] is given by

$$\phi_{i+1} = \begin{cases} \phi_i + \frac{t_\mathrm{s}}{t_\mathrm{e}} + 1 - f(\phi_i + \frac{t_\mathrm{in}}{t_\mathrm{e}}) & 0 \leq \phi_i < \frac{t_\mathrm{out}}{t_\mathrm{e}}, \\ \phi_i + \frac{t_\mathrm{s}}{t_\mathrm{e}} & \frac{t_\mathrm{out}}{t_\mathrm{e}} \leq \phi_i < \frac{t_\mathrm{out}+t_\mathrm{s}-\theta}{t_\mathrm{e}}, \\ \phi_i + \frac{t_\mathrm{s}}{t_\mathrm{e}} + 1 - f(\phi_i + \frac{t_\mathrm{in}}{t_\mathrm{e}}) & \frac{t_\mathrm{out}+t_\mathrm{s}-\theta}{t_\mathrm{e}} \leq \phi_i < 1, \end{cases} \tag{C1}$$

where ϕ_i is the phase of the ith sinus beat in the ectopic cycle. These equations can be simplified by setting

$$\tilde{\phi}_i = \phi_i - \frac{t_\mathrm{out}}{t_\mathrm{e}}, \tag{C2}$$

which yields

$$\tilde{\phi}_{i+1} = \begin{cases} \tilde{\phi}_i + \frac{t_\mathrm{s}}{t_\mathrm{e}} & 0 \leq \tilde{\phi}_i < \frac{t_\mathrm{s}-\theta}{t_\mathrm{e}}, \\ \tilde{\phi}_i + \frac{t_\mathrm{s}}{t_\mathrm{e}} + 1 - f(\tilde{\phi}_i + \frac{t_\mathrm{lag}}{t_e}) & \frac{t_\mathrm{s}-\theta}{t_\mathrm{e}} \leq \tilde{\phi}_i < 1 \end{cases} \tag{C3}$$

where $t_\mathrm{lag} = t_\mathrm{in} + t_\mathrm{out}$. Hence, the dynamics are only dependent on the *sum* of the conduction time into and out of the ectopic focus. The shifted phase $\tilde{\phi}$ can be thought of as the phase of a sinus beat in the ectopic cycle, where the ectopic cycle is shifted by t_out to account for the time between depolarization of the ectpoic focus and an ectopic beat. In the manuscript, we drop the tilde notation.

ACKNOWLEDGMENTS

This research was enabled in part by cloud services and support provided by Calcul Québec (www.calculquebec.ca) and the Digital Research Alliance of Canada (www.alliancecan.ca). GB thanks NSERC for research support. We thank the Fonds de Recherche du Quebec Nature et technologies (FRQNT) for postdoctoral support for TB. AS thanks the CIHR Canadian Institutes of Health Research (CIHR) grant (#PJT-169008).

DATA AVAILABILITY STATEMENT

The data that support the findings of this study are available on request from the corresponding author.

[1] J. A. Gomes, *Heart Rhythm Disorders: History, Mechanisms, and Management Perspectives* (Springer Nature, 2020).
[2] G. M. Marcus, "Evaluation and management of premature ventricular complexes," Circulation **141**, 1404–1418 (2020).
[3] R. Latchamsetty and F. Bogun, "Premature ventricular complexes and premature ventricular complex induced cardiomyopathy," Curr. Probl. Cardiol. **40**, 379–422 (2015).
[4] A. K. Lee, J. Andrade, N. M. Hawkins, G. Alexander, M. T. Bennett, S. Chakrabarti, Z. W. Laksman, A. Krahn, J. A. Yeung-Lai-Wah, and M. W. Deyell, "Outcomes of untreated frequent premature ventricular complexes with normal left ventricular function," Heart **105**, 1408–1413 (2019).

[5]D. S. Echt, P. R. Liebson, L. B. Mitchell, R. W. Peters, D. Obias-Manno, A. H. Barker, D. Arensberg, A. Baker, L. Friedman, H. L. Greene, *et al.*, "Mortality and morbidity in patients receiving encainide, flecainide, or placebo: the cardiac arrhythmia suppression trial," N. Engl. J. Med. **324**, 781–788 (1991).

[6]D. Steven, K. C. Roberts-Thomson, J. Seiler, K. Inada, U. B. Tedrow, R. N. Mitchell, P. S. Sobieszczyk, A. C. Eisenhauer, G. S. Couper, and W. G. Stevenson, "Ventricular tachycardia arising from the aortomitral continuity in structural heart disease: characteristics and therapeutic considerations for an anatomically challenging area of origin," Circulation: Arrhythmia and Electrophysiology **2**, 660–666 (2009).

[7]M. Levy, D. Adler, and J. Levy, "Three variants of concealed bigeminy." Circulation **51**, 646–655 (1975).

[8]M. N. Levy, I. Mori, and N. Kerin, "Two variants of concealed trigeminy," Am. Heart J. **93**, 183–188 (1977).

[9]A. Pick and R. Langendorf, *Interpretation of complex arrhythmias* (Lea & Febiger, 1979).

[10]R. Langendorf, A. Pick, and M. Winternitz, "Appearance of ectopic beats dependent upon length of the ventricular cycle, the "rule of bigeminy."," Circulation **11**, 422–430 (1955).

[11]C. Antzelevitch, M. J. Bernstein, H. N. Feldman, and G. K. Moe, "Parasystole, reentry, and tachycardia: a canine preparation of cardiac arrhythmias occurring across inexcitable segments of tissue." Circulation **68**, 1101–1115 (1983).

[12]G. Moe, J. Jalife, W. Mueller, and B. Moe, "A mathematical model of parasystole and its application to clinical arrhythmias." Circulation **56**, 968–979 (1977).

[13]J. Jalife and G. K. Moe, "Effect of electrotonic potentials on pacemaker activity of canine purkinje fibers in relation to parasystole." Circ. Res. **39**, 801–808 (1976).

[14]A. L. Wit, "Afterdepolarizations and triggered activity as a mechanism for clinical arrhythmias," Pacing and Clinical Electrophysiology **41**, 883–896 (2018).

[15]S. Akselrod, D. Gordon, F. A. Ubel, D. C. Shannon, A. Berger, and R. J. Cohen, "Power spectrum analysis of heart rate fluctuation: a quantitative probe of beat-to-beat cardiovascular control," Science **213**, 220–222 (1981).

[16]C.-K. Peng, S. Havlin, H. E. Stanley, and A. L. Goldberger, "Quantification of scaling exponents and crossover phenomena in nonstationary heartbeat time series," Chaos **5**, 82–87 (1995).

[17]M. Kawamura, N. Badhwar, V. Vedantham, Z. H. Tseng, B. K. Lee, R. J. Lee, G. M. Marcus, J. E. Olgin, E. P. Gerstenfeld, and M. M. Scheinman, "Coupling interval dispersion and body mass index are independent predictors of idiopathic premature ventricular complex-induced cardiomyopathy," Journal of cardiovascular electrophysiology **25**, 756–762 (2014).

[18]D. Hamon, P. S. Rajendran, R. W. Chui, O. A. Ajijola, T. Irie, R. Talebi, S. Salavatian, M. Vaseghi, J. S. Bradfield, J. A. Armour, *et al.*, "Premature ventricular contraction coupling interval variability destabilizes cardiac neuronal and electrophysiological control: insights from simultaneous cardioneural mapping," Circulation: Arrhythmia and Electrophysiology **10**, e004937 (2017).

[19]C. Lerma, A. Gorelick, R. N. Ghanem, L. Glass, and H. V. Huikuri, "Patterns of ectopy leading to increased risk of fatal or near-fatal cardiac arrhythmia in patients with depressed left ventricular function after an acute myocardial infarction," Europace **15**, 1304–1312 (2013).

[20]E. H. Simpson, "The interpretation of interaction in contingency tables," Journal of the Royal Statistical Society: Series B (Methodological) **13**, 238–241 (1951).

[21]L. H. Frame and M. B. Simson, "Oscillations of conduction, action potential duration, and refractoriness. a mechanism for spontaneous termination of reentrant tachycardias." Circulation **78**, 1277–1287 (1988).

[22]F. M. Weber, A. Luik, C. Schilling, G. Seemann, M. W. Krueger, C. Lorenz, C. Schmitt, and O. Dossel, "Conduction velocity restitution of the human atrium—an efficient measurement protocol for clinical electrophysiological studies," IEEE Transactions on Biomedical Engineering **58**, 2648–2655 (2011).

[23]A. Shrier, H. Dubarsky, M. Rosengarten, M. Guevara, S. Nattel, and L. Glass, "Prediction of complex atrioventricular conduction rhythms in humans with use of the atrioventricular nodal recovery curve." Circulation **76**, 1196–1205 (1987).

[24]M. Boyett and B. Jewell, "A study of the factors responsible for rate-dependent shortening of the action potential in mammalian ventricular muscle." The Journal of physiology **285**, 359–380 (1978).

[25]M. Guevara, G. Ward, A. Shrier, and L. Glass, "Electrical alternans and period doubling bifurcations," IEEE Comp. Cardiol **562**, 167–170 (1984).

[26]J. Sun, F. Amellal, L. Glass, and J. Billette, "Alternans and period-doubling bifurcations in atrioventricular nodal conduc," J. Theor. Biol. **173**, 79–91 (1995).

[27]L. Glass, A. Goldberger, and J. Belair, "Dynamics of pure parasystole," Am. J. Physiol. Heart Circ. Physiol. **251**, H841–H847 (1986).

[28]K. Diagne, T. M. Bury, M. W. Deyell, Z. Laksman, A. Shrier, G. Bub, and L. Glass, "Rhythms from two competing periodic sources embedded in an excitable medium," Physical Review Letters **130**, 028401 (2023).

[29]M. R. Guevara, L. Glass, and A. Shrier, "Phase locking, period-doubling bifurcations, and irregular dynamics in periodically stimulated cardiac cells," Science **214**, 1350–1353 (1981).

[30]M. Courtemanche, L. Glass, M. D. Rosengarten, and A. Goldberger, "Beyond pure parasystole: promises and problems in modeling complex arrhythmias," Am. J. Physiol. Heart Circ. Physiol. **257**, H693–H706 (1989).

[31]V. Schulte-Frohlinde, Y. Ashkenazy, P. C. Ivanov, L. Glass, A. L. Goldberger, and H. E. Stanley, "Noise effects on the complex patterns of abnormal heartbeats," Phys. Rev. Lett. **87**, 068104 (2001).

[32]N. Ikeda, S. Yoshizawa, and T. Sato, "Difference equation model of ventricular parasystole as an interaction between cardiac pacemakers based on the phase response curve," J. Theor. Biol. **103**, 439–465 (1983).

[33]K. Takayanagi, K. Tanaka, H. Kamishirado, Y. Sakai, T. Fujito, T. Inoue, T. Hayashi, S. Morooka, and N. Ikeda, "Direct discrimination and full-day disclosure of ventricular parasystole on new heart rate tachograms," J. Cardiovasc. Electrophysiol. **11**, 168–177 (2000).

[34]K. Takayanagi and Y. Sakai, "Mechanism of ventricular premature contraction showing interpolated bigeminy—strong modulation hypothesis—," J Arrhythm **25**, 177–192 (2009).

[35]T. Bury, C. Lerma, G. Bub, Z. Laksman, M. Deyell, and L. Glass, "Long ECGs reveal rich and robust dynamical regimes in patients with frequent ectopy," Chaos: An Interdisciplinary Journal of Nonlinear Science **30**, 113127 (2020).

[36]B. I. Sasyniuk, M. Valois, and W. Toy, "Recent advances in understanding the mechanisms of drug-induced torsades de pointes arrhythmias," The American journal of cardiology **64**, J29–J32 (1989).

[37]B. P. Damiano and M. R. Rosen, "Effects of pacing on triggered activity induced by early afterdepolarizations." Circulation **69**, 1013–1025 (1984).

[38]G. B. Nam, K. J. Choi, D. W. Park, J. Kim, K. S. Rhee, and Y. H. Kim, "Electrophysiological characteristics of arterially-perfused canine pulmonary veins: role of the delayed afterdepolarization-induced triggered activity," Korean Circulation Journal **35**, 643–648 (2005).

[39]J. Tomek, A. Bueno-Orovio, E. Passini, X. Zhou, A. Minchole, O. Britton, C. Bartolucci, S. Severi, A. Shrier, L. Virag, *et al.*, "Development, calibration, and validation of a novel human ventricular myocyte model in health, disease, and drug block," Elife **8**, e48890 (2019).

[40]D. Guo, Q. Liu, T. Liu, G. Elliott, M. Gingras, P. R. Kowey, and G.-X. Yan, "Electrophysiological properties of hbi-3000: a new antiarrhythmic agent with multiple-channel blocking properties in human ventricular myocytes," Journal of cardiovascular pharmacology **57**, 79–85 (2011).

[41]C. Antzelevitch, A. Burashnikov, and J. M. Di Diego, "Mechanisms of cardiac arrhythmia," Electrical Diseases of the Heart: Genetics, Mechanisms, Treatment, Prevention , 65–132 (2008).

[42]A. R. Pérez-Riera, R. Barbosa-Barros, N. Samesina, C. A. Pastore, M. Scanavacca, R. Daminello-Raimundo, L. C. de Abreu, K. Nikus, and P. Brugada, "Andersen–Tawil syndrome: A comprehensive review," Cardiology in Review **29**, 165–177 (2021).

[43]E. Lepeschkin and M. B. Rosenbaum, "Coupling intervals of ventricular extrasystoles in relation to the heart rate, the U wave, and the supernormal phase of excitability," Circulation **15**, 82–89 (1957).

[44]C. Lerma, C. F. Lee, L. Glass, and A. L. Goldberger, "The rule of bigeminy revisited: analysis in sudden cardiac death syndrome," J. Electrocardiol. **40**, 78–88 (2007).

[45]H. Akaike, "Information theory and an extension of the maximum likelihood principle," in *Selected papers of hirotugu akaike* (Springer, 1998) pp. 199–213.

[46]R. A. Gordon, *Regression analysis for the social sciences* (Routledge, 2015).